Annu. Rev. Physiol. 1995. 57:635–57

MUCIN BIOPHYSICS

Rama Bansil[1], *Eugene Stanley*[1], *and J. Thomas LaMont*[2]
[1]Center for Polymer Studies and Department of Physics, Boston University, Boston, Massachusetts 02215; [2]Section of Gastroenterology, Evans Department of Clinical Research, Boston University School of Medicine, Boston, Massachusetts 02118

KEY WORDS: gelation, viscoelasticity, light scattering, viscous fingering, diffusion in mucus

INTRODUCTION

Mucus, the slimy, viscous secretion that covers epithelial surfaces throughout the body, contains water, salts, immunoglobulins, secreted proteins, and mucin. Mucus secretions are thought to have important protective and lubricative properties, primarily owing to their ability to form a gel layer adherent to the underlying epithelium. Specialized epithelial cells called mucus or goblet cells secrete mucus, which adheres to the epithelial surface and forms a protective diffusion barrier between the lumen and the cell surface. The most abundant macromolecule in mucus is mucin, the general term for members of a closely related family of glycoproteins found in mucus secretions. Mucins can be defined structurally as large (M_r 10^6–10^7), viscous glycoproteins composed of approximately 75% carbohydrate and 25% amino acids linked via *O*-glycosidic bonds between *N*-acetylgalactosamine and serine or threonine residues. The purpose of our review is to describe the physical-chemical properties of epithelial mucins, particularly those that relate to aggregation or polymerization, sol-gel transition, and viscosity, because these properties appear to underlie physiological function. Where possible, we assign specific biophysical functions (e.g. molecular shape, aggregation properties, behavior at low pH) to known structural domains on the mucus molecule.

Molecular Architecture of Epithelial Mucins

The basic architecture of a typical epithelial mucin is shown in Figure 1 (84); a mucin monomer represents the entire secreted peptide encoded by mucin mRNA and synthesized by a mucus cell. Mucins are elongated rod-shaped molecules

0066–4278/95/0315–0635$05.00

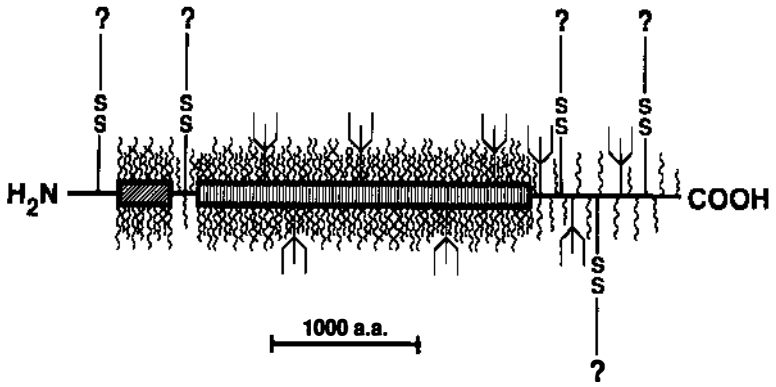

Figure 1 Schematic of intestinal mucin. The amino terminus is on the left, carboxyl on right. A cysteine-rich region occupies the last of the carboxyl end of the molecule. The glycosylated portion is boxed and contains mostly *O*-linked oligosaccharides (*wavy vertical lines*), as well as a few *N*-linked oligosaccharides (*tridents*). Whether the SS bridges are intra- or intermolecular is still open to question. (from *J. Clin. Invest.* 1991. 88:1012. Copyright permission Am. Soc. Clin. Invest.).

whose central core is a linear polypeptide (100 to 250 kDa) called apomucin (81). The unglycosylated peptide or apomucin does not exist as such in mucus or goblet cells because native mucins isolated from body secretions or tissues are always heavily glycosylated. Oligosaccharide side chains are attached by *O*-glycosidic linkage to serine and threonine residues that account for up to one-third of the amino acids in the glycosylated region. Mucin oligosaccharides of 2 to 12 monosaccharide residues may be linear or branched and project ra- dially from the peptide core. Glycosylated regions of apomucin are generally encoded by tandem repeats of DNA that encode from 6 to 169 amino acids (37). Tandem repeats are linked together in arrays up to 100 repeating units to give long glycosylated regions with total M_r of 10^6 kDa.

The nonglycosylated regions of apomucin do not contain tandem repeats, have fewer serines and threonines, and are enriched in cysteine. These regions are often at the amino or carboxyl terminals of apomucin (Figure 1) and resemble typical globular proteins as regards amino acid composition and folding. The large size of mucin genes (up to 30 kb) and the presence of glycosylated tandem repeats have slowed progress in cloning mucin DNA. At present only partially cloned sequences are available. However, full-length sequences of *MUC2* and possibly other mucin genes, including up-stream regulatory sequences, will be published within a year or two.

Function of Mucin Domains

What functions are subserved by the glycosylated and nonglycosylated domains of mucin? Early biochemical analysis (50) suggested that a separate

peptide (link peptide) cross-linked monomers in rat intestinal mucin, but recent DNA sequence data indicate that the link peptide is an integral part of apomucin, not a separate protein (91). The importance of the cysteine-rich regions in polymerization has been deduced by loss of viscous- and gel-forming properties after treatment of mucins with proteolytic enzymes that attack only the cysteine-rich regions, or by exposure to reducing agents such as dithiothreitol that disrupt disulfide bonds (81). The protease-sensitive portion of rat intestinal mucin contains a repetitive element of approximately 350 amino acids with considerable sequence homology to von Willebrand factor, a serum protein important in blood coagulation (92). These cysteine-rich motifs in von Willebrand factor are involved in oligomerization, and the presence of similar cysteine-rich motifs in human intestinal mucin (38) and human tracheobroncheal mucin (52) suggests a similar function in mucin aggregation. However, as discussed below, the disulfide bonds in mucin may be primarily intramolecular, and their function may be to provide a suitable conformation that allows cross-linking of monomers by noncovalent bonds.

The function of the glycosylated tandem repeats has been studied extensively in ovine submaxillary mucin, a salivary glycoprotein with simple disaccharides of sialic acid GalNAc. Light scattering and circular dichroism studies of native and glycosidase-treated salivary mucin revealed that GalNAc residues attached to threonine on the peptide core are essential in maintaining a highly extended random coil configuration (33, 69). Removal of all disaccharides led to collapse or denaturation of the molecule. Sialic acid residues played only a minor role in maintaining the extended configuration of the molecule. Since deglycosylated mucin (or apomucin) is insoluble in water, the oligosaccharides allow hydration of the molecule and contribute to gel formation by binding water.

The function of the more complex oligosaccharides on typical epithelial mucins has not been carefully studied. General properties of mucin-bound carbohydrates include protease resistance, large water–holding capacity and high charge density from sialic acid and sulfate residues, which are charged at neutral pH. The remarkable complexity of mucin oligosaccharides has hindered detailed assessment of their properties. For example, the major human colonic mucin species contains 21 separate oligosaccharide groups ranging in size from 2 to 12 sugar residues (60, 61); many of these oligosaccharides represent minor variations of a basic biantennary structure.

Models of Mucin Polymerization and Gelation

The interactions of mucin are responsible for structural organization at several length scales, ranging from intramolecular interactions at the level of isolated apomucin molecules, to intermolecular interactions that give rise to supramolecular aggregates and eventually the visco-elastic characteristics of the mucus

gel. Mucin monomers (Figure 1) form large aggregates in solution that take the form of extended rods or threads. For example, electron microscopy of purified pig gastric mucin reveals linear structures 5 nm in diameter and ranging in length from 100 to 5000 nm (68). Similar size ranges were observed for human cervical and tracheobronchial mucins (68), which indicates that mucins from different organs and species have a similar general structure. Considerable flexibility of mucin threads was suggested by the appearance of loops, kinks, and turns. Although the preparation of mucin for electron microscopy involved denaturing solvents, no globular or folded structures have been described, although indirect evidence suggests that the cysteine-rich, nonglycosylated portions of mucin are folded as globular polypeptides. Human cervical mucin ($M_r \sim 10^7$) can be dissociated in reducing agents to form monomers or subunits ($M_r \sim 2 \times 10^6$). Exhaustive trypsin digestion of subunits produces T domains ($M_r \sim 4 \times 10^5$), large glycopeptides that consist mostly of tandem repeats with little or no naked peptide. Monomers of cervical mucin have an average length of about 390–460 nm, and T domains of 90–100 nm by electron microscopy (67), which suggests that monomers are assembled from subunits joined end-to-end by thiol-dependent associations.

Mucin molecules in solution can cross-link to form aggregates via H-bonds, and electrostatic and hydrophobic interactions, as well as via weak Van der Waals forces. Increasing the number of cross-links leads to the formation of a gel, wherein a sufficient number of the polymers are connected to form a network that extends over the sample. At the sol-gel transition, the solution of linear or branched polymeric molecules exhibits a transition from a fluid with a finite viscosity and zero elasticity to a gel with infinite viscosity and finite elasticity (21, 28). The concentration at which the sol-gel transition occurs depends on the molecular weight of the polymer, the fraction of cross-linkable groups per polymer, and external variables such as temperature, pH, or ionic strength, which affect cross-link formation. If the cross-links are covalent, aggregation and gelation are irreversible, whereas if the cross-links are noncovalent, they will break and reform (i.e. exist in chemical equilibrium), in which case aggregation/gelation is reversible. Which interactions are involved in the aggregation/gelation of mucin and whether the gel is reversible or irreversible are still open questions.

Silberberg has proposed one hypothesis for polymerization with covalent cross-link formation that involves lectin-like binding between terminal cysteine-rich regions of one monomer with a specific sugar sequence on an adjacent monomer (72). In this model, intramolecular disulfide bonds fold the apomucin in such a way that it possesses specific lectin activity; reducing agents allow this region to unfold with loss of lectin activity and the ability to polymerize. The carbohydrate recognition site for the lectin must not occur too frequently in the tandem repeat section of mucin because too many lectin-binding sites

would allow condensation of molecules into highly aggregated clumps. The lectin polymer model is consistent with certain features of mucin solution behavior and requires that only one end of the mucin subunit contains the cysteine-rich globular sequence required for lectin activity. However, the primary structure of human intestinal mucin, as recently deduced from cDNAs (38), suggests that both amino and carboxyl terminals of mucin contain cysteine residues that participate in forming intramolecular disulfide bridges. These bifunctional mucin subunits could theoretically form disulfide bonds at either the amino or carboxyl terminus, thereby leading to formation of extended chains or threads. However, we favor the hypothesis that noncovalent bonds are involved in gelation and that intramolecular disulfide bridges provide the necessary configuration for the formation of extended head-to-tail linear polymers (13).

There are several mechanisms by which noncovalent bonds lead to reversible gelation, also called physical gelation (10). These include (*a*) gelation by the formation of secondary bonds in entangled polymer solutions, (*b*) gelation by the formation of locally ordered junction zones as in polysaccharide gels (62), and (*c*) gelation caused by differing solvent affinities of the different blocks of a multiblock copolymer (34, 35).

The idea that gelation of mucin can arise from its entanglement properties has been discussed by several authors (13, 86). High molecular weight polymer solutions are considered dilute if the individual chains do not overlap and semi-dilute beyond a concentration called the overlap concentration c^*, at which the chains just begin to overlap (21). At concentrations $c > c^*$ the solution also exhibits viscoelastic behavior due to the presence of transient entanglements. However, these polymers will eventually flow when subjected to external forces. If the polymer can form noncovalent interactions, then semi-dilute and concentrated solutions will also display rheological behavior characteristic of aggregates and eventually of reversible gelation (10). Because mucin has a very high molecular weight, its overlap concentration is very low, and mucin solutions at concentrations 2–4 mg/ml (approx1 μm) are already in the semi-dilute regime where polymer chains are overlapped. At the much higher concentrations typically found in vivo (>20 mg/ml) (1), the extensively entangled monomers will behave like a transient gel. Such close contact between neighboring molecules greatly increases the formation of noncovalent interactions that stabilize the entangled network and gives it the rheological characteristics of a weak, reversible gel.

The cross-linking of many biological gels is due to the formation of locally ordered regions involving the cooperative interactions of several weak bonds in a localized region, called the junction zone (10, 62). Although each individual bond may have an energy comparable to kT, the energy due to thermal fluctuations and cooperative interactions of multiple bonds in these junction

zones can provide the energy to stabilize the gel network. For example, gelatin and polysaccharide gels (62) are stabilized by helical junction zones, whereas physical gels of synthetic, atactic polystyrene involve the formation of microcrystalline regions (36). Whether mucin gelation involves the formation of junction zones remains a question because neither thermodynamic studies of mucin gelation nor X-ray or neutron diffraction studies of local order have been reported.

The possibility that mucin gels involve solvent-mediated interactions arises because the glycosylated regions are hydrophilic, whereas nonglycosylated sections are rich in hydrophobic amino acids (76). The differing affinities of these two domains for water can lead to physical gelation by a mechanism similar to that seen in synthetic multiblock copolymers (34); these are linear polymers made of two different polymeric blocks A and B linked covalently to form a tri-block polymer (ABA) or a multiblock polymer $(AB)_n$ with $n > 2$. In a solvent that is poor for the A block but good for the B block, the A blocks of neighboring polymers tend to associate by excluding the solvent. The B blocks act as bridges to link the domains formed by A blocks, which leads eventually to the formation of a physical gel. Such gels have been seen in several synthetic multiblock copolymers (34, 35). If this mechanism plays a role in mucin gelation, then gel formation would require intact nonglycosylated regions; this is consistent with the observation that mucin does not gel when the nonglycosylated regions are disrupted either by disulfide bond reduction or by peptide bond–breaking enzymes (1, 9, 13).

Techniques to Study Biophysical Properties of Mucin

The structure and dynamics of mucin in solutions and gels have been investigated by light scattering (3, 11, 12, 15, 39 40, 66, 69, 70, 85), sedimentation equilibrium (40), and gel chromatography (1, 13, 40) to determine the molecular weight and size; by electron microscopy to study the shape, size, and morphology (55, 67, 68); and by viscosity measurements and dynamical mechanical measurements (rheological techniques) to determine the viscoelastic properties of mucin and mucus gels (1, 64, 73, 74). Several studies of the secondary and tertiary structure by NMR have also been reported (33, 79, 80). At present there are no reports of infrared, Raman spectroscopy, X-ray, and neutron scattering studies of mucin.

In comparing these measurements, it is important to recognize that the results depend strongly on how the material was purified. Most biophysical studies of mucin involve preparations obtained in the void volume of large-pore, gel-filtration columns, further purified by density gradient centrifugation in CsCl solutions to remove nonmucin proteins, lipids, and DNA. This yields a polydisperse sample (40) with broad distribution of high molecular weight

glycoproteins (M_r of 10^6 to 10^7). A few studies have been performed on mucins that were further fractionated into narrower M_r fractions (66, 69).

Because mucin is such a complex polymer with numerous functional groups capable of interacting via several noncovalent mechanisms, detailed quantitative interpretations of these data are extremely difficult. Models based on simpler polymers should serve only as a guide in the interpretation of these data. The best strategy to unravel the structure of mucin would be to use many different biophysical techniques on mucins subjected to a variety of biochemical treatments. In the following sections we briefly review the advantages and shortcomings of applying these techniques to mucin.

Static Light Scattering Studies of Mucin

Light scattering techniques allow estimation of M_r, size, and shape of mucin macromolecules in solution. The basic quantity measured in a static light scattering experiment is the excess intensity (I) of light scattered by a solution relative to the pure solvent at different scattering angles (θ) and concentrations (c) (16, 59). The data are plotted on the so-called Zimm plot of I^{-1} vs $q^2 + jc$, where $q = (4\pi n \sin \theta/2)/\lambda$ is the scattering vector, n the refractive index of the solvent, λ the wavelength of light, and j any conveniently chosen integer to make the magnitudes of q^2 and c comparable. By extrapolating to zero angle and zero concentration, one can determine the weight-average molecular weight of the polymer, M_r, the particle scattering function, $P(\theta)$, which depends on the shape and size of the scattering particle, and the second virial coefficient reflecting polymer-solvent interactions. Assuming a random coil conformation for mucin, it is possible to determine its radius of gyration R_g from the particle-scattering function (59).

Light scattering experiments require the preparation of dust-free solutions whose concentrations and change in refractive index of the solvent per unit concentration of the added polymer are accurately known. For mucin, values of the refractive index increment have been reported to range from 0.101 ml/g for cervical mucin (12), 0.125 ml/g for ovine submaxillary mucin (69), to 0.14 ml/g for respiratory mucin (15). Because the calculation of M_r depends on $(dn/dc)^2$, a 10% error in this quantity produces a 20% error in M_r; thus it is best to measure dn/dc with a differential refractometer for the sample being studied. Polydispersity in the mucin preparation will strongly affect the determination of molecular weight because light scattering measures the average $\Sigma N_i m_i^2 / \Sigma N_i m_i$ where N_i and m_i denote the number and mass of the i^{th} species in the mixture, e.g. a 1:9 mixture of 10^7 and 2×10^6 K molecules will lead to an effective M_r of 4.9×10^6. Thus measurements on very dilute solutions (<1 mg/ml) of mucin separated into narrow molecular weight fractions are the most reliable. Several light scattering studies of mucins have been reported including submaxillary mucin (69, 70, 85), respiratory mucins (15, 39, 66), human

cervical mucin (12), intestinal mucin (11), and gastric mucin (3). These studies give M_r ranging from 1–15 million and R_g from 50–200 nm.

A scaling relation $R_g = R_0 M_r^{\alpha}$ provides an overall characterization of the shape of a polymeric molecule; $\alpha = 0.33$ for a sphere, 0.5–0.6 for a random coil, and 1 for a rigid rod (24, 72). Several authors have studied this scaling relationship for mucin (12, 15, 39, 45, 69) and find that the exponent $\alpha \approx 0.55$ is characteristic of a somewhat stiff random coil; in contrast to $\alpha \sim 0.33$ for globular proteins (45, 51). Proteins denatured in guanidine HCl show $\alpha \sim 0.5$, but the constant that is a measure of the size of the statistical segment is about seven times larger in mucin than in denatured random coil proteins (45), which indicates that on a short-length scale, mucin is much stiffer. Most likely this stiffness is related to the clustering of oligosaccharide side chains in heavily glycosylated regions. This conclusion is also supported by measurements of $1/P(\theta)$ vs q^2, which show that the data for mucin fall between the expected values for monodisperse random coils and rigid rods (12, 15). Shogren et al (69) used the worm-like chain model to determine the dimensions of mucin from light scattering measurements. They obtained relatively high values for the persistence length (12–14 nm for submaxillary mucin). Because the persistence length is the average distance that a polymer chain traverses before a significant change in direction occurs, such high values indicate a rather stiff chain. Light scattering measurements of the second virial coefficient in mucin are not accurate because A_2 is very close to zero, and even negative values indicative of poor-solvent conditions leading to polymer aggregation have been reported (66).

Dynamic Light Scattering

The diffusion constant of polymers in solutions can be determined using the technique of quasielastic light scattering, also known as dynamic light scattering (DLS), which probes the fluctuations in the scattered intensity (16, 59). These fluctuations are caused by random movement of particles in and out of the scattering volume and can be determined by measuring the intensity autocorrelation function. For a fixed scattering angle, the characteristic time of correlation function decay is proportional to the diffusion constant of particles undergoing Brownian motion in suspension. The diffusion constant is significantly reduced if the polymer aggregates because it is proportional to the inverse of the hydrodynamic radius of the particle. Currently available digital correlators allow the measurement of diffusion constants over six or more decades, covering the range from low molecular weight proteins to sub-micron size aggregates.

Verdugo and co-workers (46) observed two diffusional modes in DLS studies of cervical mucus that suggest the existence of an entangled network, the faster mode representing the fluctuations of the average entanglement spacing, and the slower mode representing the slow diffusion of mucin aggre-

gates held together by weak noncovalent bonds. Shogren et al (70) interpreted their DLS data on salivary mucin in terms of a slow diffusive mode and a faster mode that combine the rotational diffusion with the translational diffusion. Varma et al (85) used a similar interpretation in their study of the effect of Ca on the structure of porcine submaxillary mucin. The rotational diffusion constant is best measured in a depolarized dynamic light-scattering experiment, and until such data become available with mucin, the interpretation of the fast mode as a rotation of mucin molecules remains tentative. However, the translational diffusion measurements are well established and show that in dilute solution (<2 mg/ml), mucin has a hydrodynamic size of ~65 nm for gallbladder mucin (77) and ~50–100 nm for several fractions of ovine salivary mucins (70). Steiner et al (78) showed that R_h for tracheal mucin decreased upon the addition of Ca^{2+}.

Aggregation of most mucin solutions can be observed by DLS at concentrations above 4 mg/ml. DLS studies of pig gastric mucin (9) show that diffusion constants characteristic of the native mucin ($D_t \sim 10^{-8}$ cm^2/s), and small aggregates ($D_t \sim 10^{-9}$ cm^2/s) were identified even in dilute solutions of pig gastric mucin (1 mg/ml). Very large aggregates, with D_t in the range of 10^{-10}–10^{-11} cm^2/s, were seen at pH <4 in mucin solutions of higher concentration (10 mg/ml). Such aggregation was not observed when mucin was reduced, after pronase digestion, or in high ionic strength. The diffusion constant of the units obtained after S-S bond breakage was four times faster than that of native (unreduced) mucin. The absence of large aggregates after reduction of S-S bonds implies that intramolecular S-S bonds provide the appropriate conformation that allows noncovalent interactions responsible for aggregation. The appearance of aggregates below pH 4 suggests that amino acids with pK ~4 are involved in maintaining this conformation. The nonglycosylated region of pig gastric mucin is rich in aspartate and glutamate, with pKs of 3.9 and 4.1, respectively. Perhaps the protonation of these groups decreases electrostatic repulsion of the nonglycosylated regions. By combining different biophysical techniques with specific biochemical alterations of mucin, one should be able to determine the molecular interactions responsible for aggregation.

Sedimentation Velocity and Sedimentation Equilibrium

Sedimentation velocity and equilibrium methods have proven valuable for study of biological macromolecules including mucins (40). Low-speed sedimentation equilibrium using Rayleigh interference optics is a reliable method for determination of molecular weight. Sedimentation velocity can be determined using Schlieren optics, in which macromolecular concentrations are measured in terms of refractive index increments. Sedimentation equilibrium measurements in ultra-short columns provide the second virial coefficient, a measure of solute-solvent interactions.

Sedimentation velocity and equilibrium studies show that reduction of disulfide bonds results in marked reduction in size of purified lung mucin (17). These methods have also been used to show the heterogeneity and polydispersity in purified mucin solutions. Broad distributions of the molecular weight for pig gastric mucin were reported using the sedimentation equilibrium (18) as well as sedimentation velocity method (56). Harding (40) provides a detailed review of these methods applied to mucin.

The combined results of sedimentation equilibrium and static and dynamic light scattering indicate that mucin in solution is a loosely coiled, extended molecule consisting of glycosylated and nonglycosylated regions linked linearly. Log-log plots of R_g, D_t, sedimentation coefficient s, and intrinsic viscosity vs molecular weight are all in reasonable agreement with the scaling predictions for a stiff, random coil polymer. Such a structure promotes entanglement at lower concentrations than is possible with a globular structure.

Nuclear Magnetic Resonance and Other Spectroscopic Techniques

The techniques described above are sensitive to overall molecular size and shape, but the secondary structure of the peptide backbone, the effects of glycosylation on conformation and detection of H-bonds, salt bridges, and other bonds involving specific chemical groups can only be obtained from spectroscopic techniques such as NMR, infrared and Raman spectroscopy, and circular dichroism. At present, mucin has not been examined by X-ray and neutron diffraction techniques, which are traditionally used to obtain high-resolution structural information in proteins.

^{13}C NMR studies on salivary mucins (33) and gastric mucin (80), and ^{1}H NMR on gastric mucin (79) as well as on the synthetic peptide analogue of the peptide core of the human epithelial mucin coded by the *muc*-1 gene have been reported recently (29). Earlier work (4, 9) using ^{13}C NMR spectra of pig gastric mucin showed resonances attributable to the predominant carbohydrate moieties of mucin. Sterk et al (80) used two-dimensional NMR techniques to give a more precise assignment to contributions from the peptide core as well as from the oligosaccharides. Gerken et al (33) also assigned resonances to the peptide core. In both studies, dynamics of the sugar moieties and amino acid side chains were determined from ^{13}C relaxation times (T_1 and T_2) and nuclear Overhauser effect (NOE). The dynamics in solution can be described by fast motions of glycosidic side chains and of aliphatic amino acid residues as well as by slow motion of the entire molecule (79, 80). Solid-state magic angle spinning (MAS) data (80) showed that motions of the CH_2OH groups are significantly slowed in gastric mucin gels and aggregates, which suggests that H-bonds may be responsible for the increased viscosity of mucin gels. It should be noted that the measurements (80) were performed on a very low

molecular weight fragment (M_r 18,000) obtained by reducing native mucin in mercaptoethanol; clearly results on the high molecular weight mucin are needed to understand the role of H-bonds in gastric mucin aggregation. Gerken et al (33) showed that the mobility of carbon depends on the amino acid and its glycosylation state, being less mobile in the glycosylated case. The length of the carbohydrate side chain was shown to have a lesser effect; however, this may reflect the presence of only mono- and disaccharides.

^{1}H NMR data on the low molecular weight fragment studied by Sterk (79) and a 60-amino acid synthetic polypeptide analogous to the human epithelial mucin (29) show that these fragments retain a stable ordered structure and that the protons are protected from exchange with the solvent. These data lend further support to a mucin model with a linear assembly of relatively stiff glycopeptide segments linked via flexible, naked peptide regions. Thus on a short-length scale, comparable to the size of the peptide that is coded by the tandem repeat sequences observed in most mucin genes, the mucin molecule appears ordered or stiff, whereas on a large length scale, comparable to the size of the entire molecule, it appears as a random coil polymer.

Viscoelastic Properties of Mucus Gels and Mucin Solutions

The rheological properties of a polymer solution or gel are characterized by the parameters of viscosity and elasticity (27, 71). At the sol-gel transition, the viscosity becomes infinite and the network in the gel provides resistance to elastic deformations. A force applied at any point on the surface of the gel sample will be transmitted through the network and will deform it until the applied stresses are balanced by the stress induced in the network strands. The rheological characteristics of mucus and reconstituted mucins can range from those of a highly viscous solution to a true gel, depending on the source of mucus, and experimental and physiological variables such as pH, ionic strength, and the presence of other molecules (73).

The viscosity of mucin solutions is related to its functional properties and changes with variation of mucin molecular weight as well as its state of aggregation. For example, oral mucus of caries-resistant individuals has lower viscosity than that of caries-susceptible individuals owing to variation in the mucin molecular size and the bound lipid content of mucus secretions (75). Aggregation of pig gastric mucus at low pH and low ionic strength is reflected by at least 100-fold increases of viscosity measured by the falling ball technique (9). Intrinsic viscosity measurements in gastric mucin using capillary viscometers also show a nonlinear, asymptotic rise as a function of mucin concentration at low pH, indicative of eventual gelation at some concentration (1). Because mucin is a non-Newtonian fluid, its viscosity is strongly dependent on the shear rate (5), as revealed by several authors using cone and plate and other viscosity measurements at well-defined shear rates. Apparent vis-

cosity of frog epithelial mucus increases by one order of magnitude as the shear rate decreases from 1–0.1 s^{-1} (74), a characteristic of a weak visco-elastic material close to the sol-gel transition.

The mechanical properties of a weak viscoelastic gel (32) are characterized by two parameters, G' and G''; the degree of solid-like behavior reflected by the storage or elastic modulus (G') and the liquid-like properties by the loss or viscous modulus (G''). A viscoelastic material is more viscous below the sol-gel transition ($G'' > G'$), whereas above the transition, it is more elastic ($G' > G''$). Thus the incipient gel can be identified as just forming at the sol-gel transition by the condition that $G' = G''$. The quantity $\tan \delta = G''/G'$ is a measure of the gel strength. The response of these two moduli to shear frequency provides a measure of how the gel responds to shear forces generated by fluid flow. This property is of obvious relevance to the ability of intestinal mucus to withstand the large shear forces found in the digestive tract and to the movement of particles over the epithelial surface. The gel acts as a mechanical coupler.

Under certain conditions, native mucus and purified mucin exhibit several of the gel-like properties mentioned above (64, 73). Native bovine cervical mucus at midcycle has rheological characteristics that are similar to an incipient gel at the threshold of the sol-gel transition with $G' = G''$ (32). Scanning electron microscopic studies of cervical mucus reveal a filamentous three-dimensional network with pores or channels (55). The size of channels and filaments appears to depend on the estrus cycle, with the average spacing being smaller in the progestational state and larger in midcycle. The mechanical spectra of native mucus gels and purified mucin at physiological concentrations (20–50 mg/ml, depending on the source of the mucin) are similar. At these concentrations, the materials are clearly gels with the storage modulus $G' > G''$, and $\tan \delta \sim 0.4$–0.2 (6, 65). In contrast, S-S reduced mucin or proteolytically digested mucin have $\tan \delta \sim 2$–4, which indicates an inability to form a gel (1, 6). Respiratory mucus and mucin also show similar mechanical properties characteristic of weak viscoelastic gels. Whereas mucus and reconstituted mucin gels are usually weak with low values of G', considerable strengthening of gels occurs, as reflected by an increase in G', when mucoadhesive polymers such as polyacrylic acid are added to mucin (53).

Swelling Behavior of Mucus Gels

Mucus is 80 to 90% hydrated, thus the swelling behavior of mucin gels is highly relevant to their physiological function. A covalently cross-linked gel will swell to an equilibrium limit, depending on the elasticity of the network, rather than dissolve upon the addition of more solvent (28). Gels whose molecules are capable of electrostatic interactions can swell as much as a thousandfold (47). A reversible gel will not swell on addition of further solvent

because the sol-gel transition in these gels depends on polymer concentration. Such a gel will eventually dissolve upon dilution, although the dissolution process may be very slow. Swelling behavior ranges from no further swelling to swelling enormously depending on the source of mucus, its freshness, and the method of preparation of mucin (73). Because mucins are polyanions, their swelling is governed by a Donnan equilibrium arising from the competing effects of electrostatic repulsions of negative charges on the polyanion and attractive interactions of free cations with fixed negative charges (83). This phenomenon explains the dependence of the degree and rate of swelling on pH and ionic strength. Donnan effects also provide a mechanism for the storage in goblet cells of a condensed network of mucin that swells extensively upon secretion, as evidenced by video microscopy (86).

Diffusion of Macromolecules Through Mucus and Mucin Gels

The presence of a mesh or compartments in a gel significantly retards the diffusional movement of other macromolecules through it (21, 24, 57). The diffusion constant depends on the relative size of diffusant and the mesh size of the gel. Macromolecules larger than the correlation length of the gel lose their lateral mobility and diffuse very slowly by a process called reptation (21, 24), whereas smaller molecules can diffuse laterally as well. Molecules and particles that are much larger than the mesh size of the gel may be immobilized in the gel. The diffusion coefficients of several macromolecules of varying molecular weight through native porcine mucus are reduced by a factor ranging from 10 to 30 as compared with the diffusion constant in aqueous solution (23). Macromolecules with M_r >30,000 were retarded more, perhaps because reptation occurs above this molecular weight. The role of mucus as a diffusional barrier to the movement of large particles depends crucially on the size of the pores in the gel. Saltzman et al (63) used electron microscopy to show that cervical mucus at midcycle has 100 nm pores, which allows antibodies and other large molecules to diffuse through the mucus, although the process is greatly slowed. Adhesive interactions between mucus and particles may be responsible for immobilization of large particles.

Hydrodynamic Properties of Mucin Gels

Among the biophysical properties of mucin that have recently received considerable attention are those related to its hydrodynamic properties when interacting with other fluids. Generically, these properties are termed viscous fingering and refer explicitly to what happens when one fluid displaces another under pressure. When the displacing fluid is more viscous than the fluid being displaced, the interface is simple; the less viscous fluid is completely displaced in a symmetric fashion. However, when the displacing fluid is less viscous, the interface between the two fluids can be complex; some of the displaced

fluid remains behind the interface in lacunae, or "fjords," as the less viscous fluid penetrates in a hierarchy of branching structures or channels, termed viscous fingers.

Exactly such viscous fingers form when HCl is injected into solutions of gastric mucin (8), raising the possibility that these channels may be relevant to the resolution of the age-old paradox concerning how acid can pass into the lumen of the stomach without simultaneously digesting the stomach itself. Indeed, physiologists have been puzzled as to why the stomach does not "digest itself" (19) ever since the 18th century scientist Ferchault de Reaumur showed that gastric juice could digest meat. The concentration of HCl in the mammalian stomach after each meal is sufficient to digest the stomach; yet, for reasons not fully understood, the gastric epithelium remains undamaged in this harsh environment.

A number of mammalian tissues (e.g. lung, stomach, intestinal, cervical) secrete mucus that forms a gel layer some 200–500 μm thick between the epithelium and the environment. Whether gastric mucus provides an effective barrier against the harsh acid environment (pH 1–2) of the stomach has been the subject of investigation for many years (2, 41, 42, 89). Early studies appeared to indicate that mucus does not have the ability to impede diffusion of hydrogen ions. The role of mucus as a barrier was considered to be more due to the presence of bicarbonate ions providing an unstirred layer trapping hydrogen ions (41). Davenport (19) suggested that the tight junctions between the epithelial cells prevented the hydrogen ions from invading the deeper mucosa, but later studies have shown that acid-induced injury to cells can occur even when the tight junctions alone are still intact, which implies that such junctions are not effective barriers to hydrogen ion diffusion.

Recent investigations indicate that solutions of gastric mucin can significantly retard diffusion of hydrogen ions (48, 58, 87, 88). Even more significantly, both in vitro and in vivo studies have demonstrated the existence of a gradient from pH 1–2 at the luminal surface to pH 6–7 at the cell surface (82, 88). It would appear that the pH gradient is maintained because hydrochloric acid, secreted by parietal cells deep in the gastric glands, somehow manages to traverse the mucus layer without gross acidification and is inhibited from diffusing back from the lumen.

How does gastric mucus support this pH gradient between lumen and mucosa and why it is not lost during active acid secretion? Until recently, little was known about how HCl secreted by parietal cells reaches the lumen. Although it is commonly accepted that mucus is a diffusion barrier for luminal acid, there is no explanation of how the acid traverses the mucus layer in the first place. Recently, Holm & Flemstrom studied HCl secretion in vivo in the rat stomach using a pH-sensitive dye (43). During active HCl secretion, they observed discrete blue spots directly above the crypts. The authors suggest

that HCl travels in channels through the mucus layer. Since mucus is considerably more viscous than HCl, Fabry (25) suggests that the hydrodynamic phenomenon of viscous fingering may be involved.

As mentioned above, the phenomenon of viscous fingering (44) explains the ability of a low viscosity fluid to pass through a fluid of higher viscosity without mixing (7, 31, 54). Depending upon the narrowness of the fingers and the size of the fjords, the driving fluid may penetrate the stationary fluid without grossly displacing it. Recently, Bhaskar et al (8) presented evidence supporting the possibility that migration of HCl through mucus may involve viscous fingering. Specifically, they demonstrated that injection of HCl into solutions of pig gastric mucin produces fingering patterns that are strongly dependent on pH and mucin concentration (Figure 2a–d). Above pH 4, discrete fingers were observed, while below pH 4, HCl neither penetrated the mucin solution nor formed fingers. These results suggest that HCl secreted under pressure by the gastric gland can penetrate the mucus gel layer (pH 5–7) through narrow fingers, whereas HCl in the lumen (pH 2) is prevented from either diffusive or convective return to the epithelium by the high viscosity of gastric mucus gel on the luminal side. Accordingly, when mucin was injected into acid, the interface was shown to be stable against perturbations and developed symmetrically (see Figure 2e). To extend the relevance of the two-dimensional viscous fingering experiments to the in vivo situation where the acid jet originates in the gastric gland and travels toward the lumen through a layer of mucus, Bhaskar et al (8) also studied acid migration through a column of mucin solution. When acid was injected into water, it diffused irregularly into the water. When HCl was injected at the same flow rate into a solution of gastric mucin, the acid traveled in a discrete plume to the top. It then layered across the top of the mucus layer and did not diffuse downward into the solution. When simultaneously injected with a pair of syringes at two ports, the acid traveled in two discrete plumes that did not intermix.

Bhaskar et al (8) hypothesized that such channels or fingers would be likely in view of the profound increase in gastric mucin viscosity at low pH. The size and shape of the fingers were found to be sensitive to concentration and pH of the mucin solution, temperature, and acid velocity. More precise characterization of the fingering patterns as a function of these physiological parameters is critical to the hypothesis that viscous fingering provides channels for secreted acid to reach the lumen without disrupting the mucus layer. If the fingering pattern consists of multiple branches with many fine "twigs" (22), a major displacement of the mucus layer would occur. By contrast, if under normal physiological conditions a single finger forms to provide a narrow channel, as suggested (8), this would not disrupt the mucus gel layer.

In summary, hydrodynamic theory implies that a low viscosity fluid (HCl, in the present case) secreted under pressure into a high viscosity fluid (gastric

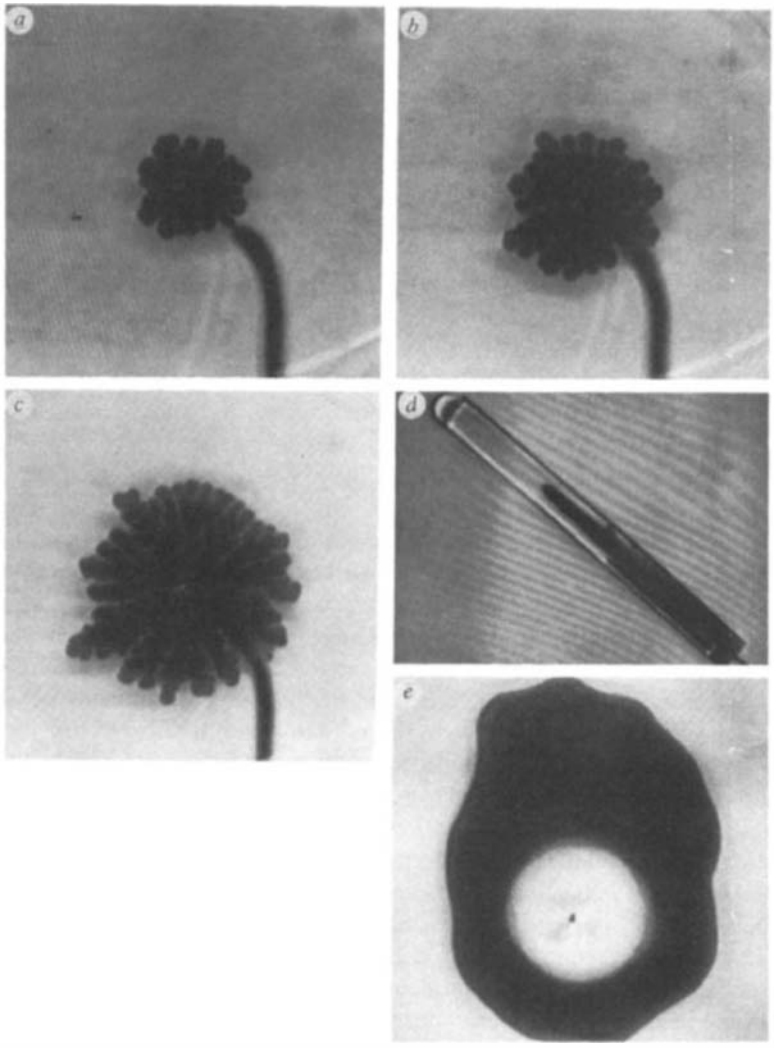

Figure 2 Viscous fingers formed by HCl (*dark*) injected into solutions of gastric mucin (*light*). The patterns were recorded with a video CCD camera. Several frames are shown: (*a-c*) fingering pattern for HCl into mucin (10 mg/ml, pH 7) at successive time intervals. For tip-splitting fingers, constant injection rate results in a decrease in interfacial velocity with time. The increase in finger packing may be due to this variation. (*d*) Single finger produced by injection of HCl (*dark*) into mucin (*light*) in the channel geometry. (*e*) Mucin (*light*) injected into HCl (*dark*) does not produce viscous fingers but rather results in complete symmetric displacement.

mucus) must display the phenomenon of viscous fingering. Viscous fingering offers a mechanism by which HCl can traverse ~500 μm of mucus between the crypt opening and the gastric lumen [and whereby a volume of 250 ml/hr of HCl (49) can pass through a much smaller protective volume of 30–50 ml of mucus] without the mucus layer suffering major disruption.

Viscous fingers are interpreted theoretically with the prototype model of diffusion limited aggregation (DLA) (90). Recently, several phenomena of biological interest including the growth of bacterial colonies (30), the retinal vasculature (26), and neuronal outgrowth (14) have attracted the attention of DLA aficionados. Like many models in statistical mechanics, the rule defining DLA is simple. At time 1, we place in the center of a computer screen a white pixel and release a random walk from a large circle surrounding the white pixel (Figure 3a). The four perimeter sites have an equal a priori probability p_i to be stepped on by the random walk; accordingly we write

$$p_i = 0.25 \ (i = 1,...,4). \qquad 1.$$

The DLA rule is that the random walker sticks irreversibly—-thereby forming a cluster of mass $M = 2$. There are $N_p = 6$ possible sites, henceforth called growth sites (Figure 3b), but now the probabilities are not all identical; each of the potential growth sites of the two tips has growth probability $p_{max} \approx 0.22$, wherease each of the four growth sites on the sides has growth probability $p_{min} \approx 0.14$. Because a side on the tip is 50% more likely to grow than a site on the sides, the next site is more likely to be added to the tip. One of the main features of modern approaches to DLA is that instead of focusing on the tips that are getting richer, the focus is on the fjords, which are getting poorer—-a

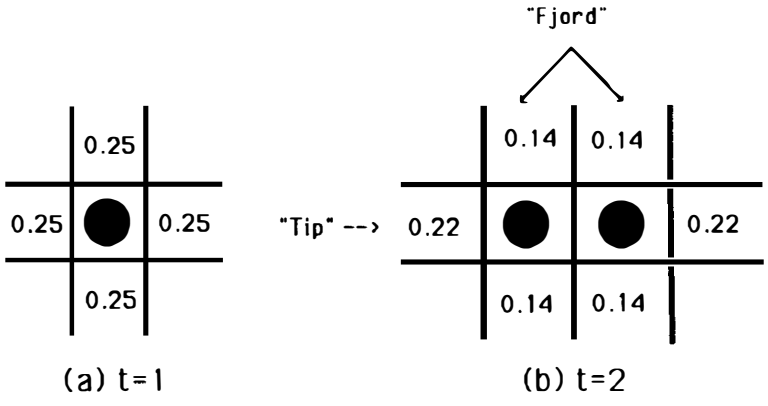

Figure 3 (a) Square lattice DLA at time t = 1, showing the four growth sites, each with growth probability $p_i = 0.25$. (b) DLA at time t = 2, with six growth sites, and their corresponding growth probabilities p_i.

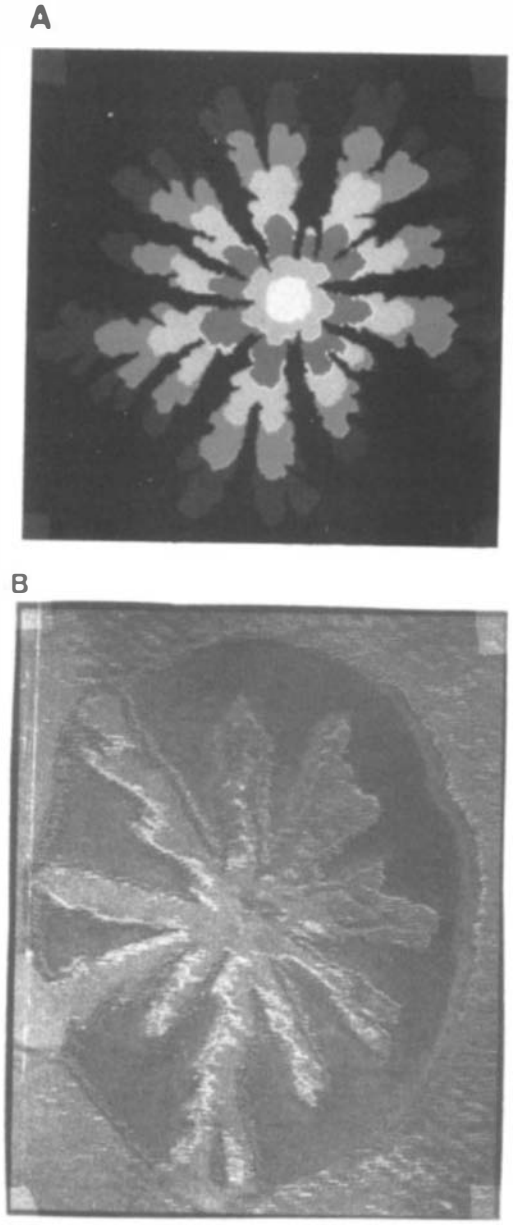

Figure 4 (*a*) Large DLA cluster on a square lattice. (*b*) Results of viscous fingering experiments of Bhaskar et al (8). In the experiment, HCl without added trypan blue was injected into mucin solution containing the acid indicator dye bromophenol blue, which turns yellow at acidic pH (color not shown in figure). The absence of changes in the color of the acid indicator dye indicates that during the passage of HCl, hydrogen ions are confined to the boundary of the fingers and do not diffuse into the mucin solution.

situation perhaps more familiar to scientists who all know the feeling that "once you get behind you stay behind!"

Although the third particle is more likely to stick at the tip, this does not mean that the next particle will stick on the tip. Indeed, the most that one can say about the cluster is to specify the growth site probability distribution, i.e. the set of numbers,

$$\{p_i\}\ i = 1...N_p, \qquad 2.$$

where p_i is the probability that perimeter site (growth site) is the next to grow, and N_p is the total number of perimeter sites ($N_p = 4,6$ for the cases $M = 1,2$ shown in Figure 1a,b, respectively). The recognition that the set of $\{p_i\}$ provides essentially the maximum amount of information about the system is connected to the fact that tremendous attention has been paid to these p_i and to the analogues of the p_i in various closely related systems.

If the DLA growth rule is simply iterated, we obtain a large cluster, from the tips to the fjords, characterized by a range of growth probabilities that spans several orders of magnitude. Figure 4a shows such a large cluster, where each pixel is colored according to the time it was added to the aggregate. From the fact that the last to arrive particles (green pixels) are never found to be adjacent to the first to arrive particles (white pixels), we conclude that the p_i for the growth sites on the tips must be vastly larger than the p_i for the growth sites in the fjords. Based on these studies, it is quite possible that DLA models what occurs when acid is forced under pressure into mucin.

ACKNOWLEDGMENT

This work was partially supported by the National Science Foundation and the National Institutes of Health. RB thanks the Bunting Institute of Radcliffe College for fellowship support.

Literature Cited

1. Allen A. 1981. Structure and function of gastrointestinal mucus. In *Physiology of the Gastrointestinal Tract,* ed. LR Johnson, 1:617–39. New York: Raven
2. Allen A, Garner A. 1980. Gastric mucus and bicarbonate secretion and their possible role in mucosal protection. *Gut* 21:249–62
3. Allen A, Mantle M, Pearson JP. 1980. The polymeric structure and properties of mucus glycoproteins. In *Perspectives in Cystic Fibrosis,* ed. J Sturgess, pp. 102–12. Toronto: Can. Cystic Fibrosis Found.
4. Barrett-Bee K, Bedford G, Loftus P. 1982. The use of natural-abundance high

resolution carbon-^{13}NMR in the study of mucus glycoproteins. *Biosci. Rep.* 2:257–63
5. Bell AE, Allen A, Morris E, Ross-Murphy S. 1984. Functional interactions of gastric mucus glycoprotein. *Int. J. Biol. Macromol.* 6:309–15
6. Bell AE, Sellers LA, Allen A, Cunliffe WJ, Morris ER, Ross-Murphy SB. 1985. Properties of gastric acid duodenal mucus; effect of proteolysis, disulfide reduction, bile, acid, ethanol and hypertonicity on mucus gel structure. *Gastroenterology* 88:269–80
7. Ben-Jacob E, Garik P. 1990. The formation of patterns in nonequilibrium growth. *Nature* 343:523–30
8. Bhaskar KR, Garik P, Turner BS, Bradley JD, Bansil R, et al. 1992. Viscous fingering of HCl through gastric mucin. *Nature* 360:458–61
9. Bhaskar KR, Gong D, Bansil R, Pajevic S, Hamilton JA, et al. 1991. Profound increase in viscosity and aggregation of pig gastric mucin at low pH. *Am. J. Physiol.* 261:G827–32
10. Burchard W, Stadler R, Freitas LL, Moller M, Omeis J, Muhleisen E. 1988. Covalent, thermoreversible and entangled network: an attempt at comparison. In *Biological and Synthetic Polymer Network,* ed. O Kramer. New York: Elsevier Appl. Sci.
11. Carlstedt I, Herrmann A, Karlsson H, Sheehan J, Fransson L-Å, Hansson GC. 1993. Characterization of two different glycosylated domains from the insoluble mucin complex of rat small intestine. *J. Biol. Chem.* 268:18771–79
12. Carlstedt I, Lindgren H, Sheehan JK. 1983. The macromolecular strucure of human cervical–mucus glycoproteins. *Biochem. J.* 213:427–35
13. Carlstedt I, Sheehan JK, Corfield AP, Gallagher JT. 1985. Mucus glycoproteins: a gel of a problem. *Essays Biochem.* 20:40–76
14. Caserta F, Stanley HE, Eldred W, Daccord G, Hausmann R, Nittmann J. 1990. Physical mechanisms underlying neurite outgrowth: a quantitative analysis of neuronal shape. *Phys. Rev. Lett.* 64:95–98
15. Chace KV, Naziruddin B, Desai VC, Flux M, Sachdev GP. 1989. Physical properties of purified human respiratory mucus glycoproteins: effects of sodium chloride concentration on the aggregation properties and shape. *Exp. Lung Res.* 15:721–37
16. Chu B. 1974. *Laser Light Scattering.* New York: Academic
17. Creeth JM, Bhaskar KR, Horton J, Das I, Lopez-Vidriero MT, Reid L. 1977. The separation and characterization of bronchial glycoproteins by density gradient methods. *Biochem. J.* 167:557–69
18. Creeth JM, Coupe B. 1984. Studies on the molecular weight distributions of two mucins. *Biochem. Soc. Trans.* 12: 618–21
19. Davenport HW. 1967. Salicylate damage to the mucosal barrier. *N. Engl. J. Med.* 23:1307–12
20. Davenport HW. 1972. Why the stomach does not digest itself. *Sci. Am.* 226:86–94
21. deGennes PG. 1979. *Scaling Concepts in Polymer Physics.* Ithaca: Cornell Univ. Press
22. deGennes PG. 1987. Time effects in viscoelastic fingering. *Europhys. Lett.* 3:195–97
23. Desai MA, Mutlu M, Vadgama P. 1992. A study of macromolecular diffusion through native porcine mucus. *Experientia* 48:22–26
24. Doi M, Edwards SF. 1986. *The Theory of Polymer Dynamics.* Oxford: Clarendon
25. Fabry TL. 1990. How the parietal secretion crosses the gastric mucus without being neutralized. *Gastroenterology* 98:A42
26. Family F, Masters BR, Platt DE. 1989. Fractal pattern formation in human retinal vessels. *Physica D* 38:98–103
27. Ferry JD. 1970. *Viscoelastic Properties of Polymers.* New York: Wiley. 2nd ed.
28. Flory PJ. 1953. *Principles of Polymer Chemistry.* Ithaca: Cornell Univ. Press
29. Fontenot JD, Tjandra N, Bu D, Ho C, Montelaro RC, Finn OJ. 1993. Biophysical characterization of one-, two-, and three-tandem repeats of human mucin (muc-1) protein core. *Cancer Res.* 53: 5386–94
30. Fujikawa H, Matsushita M. 1989. Fractal growth of *Bacillus subtilis* on agar plates. *J. Phys. Soc. Jpn.* 58: 3875–78
31. Garik P, Hetrick J, Orr B, Barkey D, Ben-Jacob E. 1991. Interfacial cellular mixing and the determination of global deposit morphology. *Phys. Rev. Lett.* 66: 1606–9
32. Gelman RA, Meyer FA. 1979. Mucociliary transference rate and mucus viscoelasticity: dependence on dynamics storage and loss modulus. *Am. Rev. Resp. Dis.* 120:553–57
33. Gerken TA, Butenhof KJ, Shogren R. 1989. Effects of glycosylation on the conformation and dynamics of O-linked glycoproteins: carbon-^{13} NMR studies

of ovine submaxillary mucin. *Biochemistry* 28:5536–43
34. Glotzer SC, Bansil R, Gallagher PD, Gyure MF, Sciortino F, Stanley HE. 1993. Physical gels and microphase separation in multiblock copolymers. *Physica A* 201:482–95
35. Guenet JM. 1992. *Thermoreversible Gelation of Polymers and Biopolymers.* New York: Academic
36. Guenet JM, Klein M, Menelle A. 1989. Evidence by neutron diffraction of ordered structures in atactic polystyrene/carbon disulfide physical gels. *Macromolecules* 22:493–94
37. Gum JR. 1992. Mucin genes and the proteins they encode: structure, diversity and regulation. *Am. J. Respir. Cell. Mol. Biol.* 7:557–64
38. Gum JR, Hicks JWQ, Torbara NW, Rothe E-M, Legace RE, et al. 1992. The human MUC-2 intestinal mucin has cysteine-rich subdomains located both upstream and downstream of its central repetitive region. *J. Biol. Chem.* 267: 21375–83
39. Gupta R, Jentoft N, Jamieson AM, Blackwell J. 1990. Structural analysis of purified human tracheobronchial mucins. *Biopolymers* 29:347–55
40. Harding SE. 1989. The macrostructure of mucus glycoproteins in solution. *Adv. Carbohydr. Chem. Biochem.* 47: 345–81
41. Heatley NG. 1959. Mucosubstance as a barrier to diffusion. *Gastroenterology* 37:313–17
42. Hollander F. 1954. Two-component mucous barrier: its activity in protecting gastroduodenal mucosa against peptic ulceration. *Arch. Int. Med.* 93:107–29
43. Holm L, Flemstrom G. 1990. Microscopy of acid transport at the gastric surface in vivo. *J. Int. Med.* 228 (Suppl.):91–95
44. Homsy GM. 1987. Viscous fingering in porous media. *Annu. Rev. Fluid Mech.* 19:271–311
45. Jentoft N. 1990. Why are proteins O-glycosylated? *Trends Biochem. Sci.* 15: 291–94
46. Lee WI, Verdugo P, Blandau RJ, Gaddum-Rosse P. 1977. Molecular arrangement of cervical mucus: a reevaluation based on laser light-scattering spectroscopy. *Gynecol. Invest.* 8:254–66
47. Li Y, Tanaka T. 1990. Swelling of gels and diffusion of molecules. In *Springer Proceedings in Physics: Dynamics and Patterns in Complex Fluids,* ed. A Onuki, K Kawasaki, 52:44–54. Berlin/ Heidelberg: Springer-Verlag
48. Lucas M. 1982. Restriction of hydrogen and sodium ion diffusion in porcine gastric mucin: a concentration dependent phenomenon. *Adv. Exp. Med. Biol.* 144:193
49. Makhlouf GM. 1981. See Ref. 1, pp. 551–66
50. Mantle M, Allen A. 1981. Isolation and characterization of the native glycoprotein from pig small intestine mucus. *Biochem. J.* 195:267–73
51. McDonnell ME, Jamieson AM. 1976. *Biopolymers* 15:1283–99
52. Meerzaman D, Charles P, Daskal E, Polymeropoulos MH, Martin BM, et al. 1994. Cloning and analysis of cDNA encoding a major airway glycoprotein, human tracheobronchial mucin (MUC-5). *J. Biol. Chem.* 269:12932–39
53. Mortazavi SA, Carpenter BG, Smart JD. 1993. A comparative study on the role played by mucus glycoproteins in the rheological behaviour of the mucoadhesive/mucosal interface. *Int. J. Pharm.* 94: 195–201
54. Nittmann J, Daccord G, Stanley HE. 1985. Fractal growth of viscous fingers: quantitative characterization of a fluid instability phenomenon. *Nature* 314: 141–44
55. Odeblad E. 1977. Physical properties of cervical mucus. In *Advances in Experimental Medicine and Biology. Mucus in Health and Disease,* ed. M Elstein, DV Parke, 89:217–25. New York: Plenum
56. Pain RH. 1980. *Symp. Soc. Exp. Biol.* 34:359–76
57. Pajevic S, Bansil R, Konak C. 1993. Diffusion of linear polymer chains in methyl methacrylate gels. *Macromolecules* 26:305–12
58. Pfeiffer CJ. 1981. Experimental analysis of hydrogen ion diffusion in gastrointestinal mucus glycoprotein. *Am. J. Physiol.* 240:G176–82
59. Phillies GD, Billmeyer FW. 1986. Elastic and quasielastic light scattering by solutions and suspensions. In *Optical Methods of Analysis,* pp. 1–87. New York: Wiley
60. Podolsky DK. 1985. Oligosaccharide structures of human colonic mucin. *J. Biol. Chem.* 260:8262–71
61. Podolsky DK. 1985. Oligosaccharide structures of human colonic mucin species. *J. Biol. Chem.* 260:15510–15
62. Rees DA. 1969. Structure, conformation, and mechanism in the formation of polysaccharide gels and networks. *Adv. Carbohydr. Chem. Biochem.* 24: 267–329
63. Saltzman WM, Radomsky ML, Whaley

KJ, Cone RA. 1994. Antibody diffusion in human cervical mucus. *Biophys. J.* 66:508–15

64. Sellers LA, Allen A. 1989. Gastrointestinal mucus gel rheology. In *Symposia of the Society for Experimental Biology XLIII: Mucus and Related Topics,* ed. E Chantler, NA Ratcliffe, pp. 65–71. Cambridge, UK: Company of Biologists
65. Sellers LA, Allen A, Morris ER, Ross-Murphy SB. 1987. Mechanical characterization and properties of gastro-intestinal mucus gel. *Biorheology* 24: 615–23
66. Shankar V, Virmani AK, Naziruddin B, Sachdev GP. 1991. Macromolecular properties and polymeric structure of canine tracheal mucins. *Biochem. J.* 276: 525–32
67. Sheehan JK, Carlstedt I. 1990. Electron microscopy of cervical-mucus glycoproteins and fragments therefrom. *Biochem. J.* 265:169–78
68. Sheehan JK, Oates K, Carlstedt I. 1986. Electron microscopy of cervical, gastric and bronchial mucus glycoproteins. *Biochem. J.* 239:147–53
69. Shogren R, Gerken TA, Jentoft N. 1989. Role of glycosylation on the conformation and chain dimensions of O-linked glycoproteins: light-scattering studies of ovine submaxillary mucin. *Biochemistry* 28:5525–35
70. Shogren R, Jamieson AM, Blackwell J, Cheng PW, Dearborn DG, Boat TF. 1983. Solution properties of porcine submaxillary mucin. *Biopolymers* 22:1657–75
71. Silberberg A. 1977. Basic rheological concepts. In *Mucus in Health and Disease,* ed. M Elstein, DV Podke, pp. 181–90. New York: Plenum
72. Silberberg A. 1987. A model for mucus glycoprotein structure. *Biorheology* 24: 605–14
73. Silberberg A. 1989. Mucus glycoprotein, its biophysical and gel-forming properties. See Ref. 64, pp. 43–63
74. Silberberg A, Meyer FA, Gilboa A, Gelman RA. 1977. Function and properties of epithelial mucus. See Ref. 55, pp. 171–80
75. Slomiany BL, Murty VLN, Mandel ID, Zalesna G, Slomiany A. 1989. Physicochemical characteristics of mucus glycoproteins and lipids of the human oral mucosal mucus coat in relation to caries susceptibility. *Arch. Oral Biol.* 34:229–37
76. Smith BF, LaMont JT. 1984. Hydrophobic binding properties of bovine gallbladder mucin. *J. Biol. Chem.* 259: 12170–77
77. Smith BF, Peetermans JA, Tanaka T, LaMont JT. 1989. Subunit interactions and physical properties of bovine gallbladder mucin. *Gastroenterology* 97: 179–87
78. Steiner CA, Litt M, Nossal R. 1984. Effect of Ca on the structure and rheology of canine tracheal mucin. *Biorheology* 21:235–52
79. Sterk H. 1988. On the structure of mucus glycoproteins: ^{1}H NMR nuclear Overhauser enhancement study. *Int. J. Biol. Macromol.* 10:213–16
80. Sterk H, Fabian W, Hayn E. 1987. Dynamic behavior of mucus glycoproteins: a ^{13}C NMR relaxation study. *Int. J. Biol. Macromol.* 9:58–62
81. Strous GJ, Dekker J. 1992. Mucin-type glycoproteins. *Crit. Rev. Biochem. Mol. Biol.* 27:57–92
82. Takeuchi K, Magee D, Critchlow J, Matthews J, Silen W. 1983. Studies of the pH gradient and thickness of frog gastric mucus gel. *Gastroenterology* 84: 331–40
83. Tam PY, Verdugo P. 1981. Control of mucus hydration as a Donnan equilibrium process. *Nature* 292:340–42
84. Toribara NW, Gum JR, Culhane PJ, Legace RE, Hicks JW, et al. 1991. *MUC-2* human small intestinal mucin gene structure, repeated arrays and polymorphism. *J. Clin. Invest.* 88:1005–13
85. Varma BK, Demers A, Jamieson AM, Blackwell J, Jentoft N. 1990. Light scattering studies of the effect of Ca on the structure of porcine submaxillary mucin. *Biopolymers* 29:441–48
86. Verdugo P. 1993. Polymer gel phase transition in condensation-decondensation of secretory products. In *Responsive Gels: Volume Transitions II,* ed. K Dusek, pp. 145–56. Berlin: Springer-Verlag
87. Williams SE, Turnberg LA. 1980. Retardation of acid diffusion by pig gastric mucus: a potential role in mucosal protection. *Gastroenterology* 79:299–304
88. Williams SE, Turnberg LA. 1981. Demonstration of a pH gradient across mucus adherent to rabbit gastric mucosa: evidence for a mucus-bicarbonate barrier. *Gut* 22:94–96
89. Williams SE, Turnberg LA. 1982. Studies of the protective properties of gastric mucus. *Adv. Exp. Med. Biol.* 144:187–88
90. Witten TA, Sander LM. 1981. Diffusion-limited aggregation, a kinetic critical phenomenon. *Phys. Rev. Lett.* 47: 1400–3
91. Xu G, Huan L-J, Khatri I, Sajjan US, McCool D, et al. 1992. Human intestinal mucin-like protein (MLP) is homologous with rat MLP in the C-terminal

region, and is encoded by a gene on chromosome 11 p 15.5. *Biochem. Biophys. Res. Commun.* 183:821–28
92. Xu G, Huan L-J, Khatri IA, Wang D, Bennick A, et al. 1992. cDNA for the carboxyl-terminal region of a rat intestinal mucin-like peptide. *J. Biol. Chem.* 267:5401–7